ASIA-PACIFIC JOURNAL OF CHEMICAL ENGINEERING
Asia-Pac. J. Chem. Eng. (2016)
Published online in Wiley Online Library
(wileyonlinelibrary.com) DOI: 10.1002/apj.2058

Curtin University

Research article

Hydrophobic-functionalized ZIF-8 nanoparticles incorporated PDMS membranes for high-selective separation of propane/nitrogen

Jianwei Yuan, Qianqian Li, Jie Shen, Kang Huang, Gongping Liu, Jing Zhao, Jingui Duan and Wanqin Jin**

State Key Laboratory of Materials-Oriented Chemical Engineering, College of Chemistry and Chemical Engineering, Nanjing Tech University, Nanjing 210009, China

Received 22 August 2016; Revised 8 October 2016; Accepted 29 October 2016

ABSTRACT: It is still a great challenge to prepare high performance mixed matrix membranes (MMMs) because of the difficulty in finely tuning the compatibility between filler and organic phases. In this work, ZIF-8 nanoparticles hydrophobically functionalized by 5, 6-dimethylbenzimidazole (DMBIM) via shell ligand exchange (SLE) reaction were incorporated into polydimethylsiloxane (PDMS) matrix to fabricate defect-free MMMs. Organic-–inorganic interface compatibility was realized because of more abundant organic ligands from DMBIM. The effects of different loadings on membrane microstructure and gas separation performance were investigated systematically. A significantly enhanced C_3H_8/N_2 separation performance with C_3H_8 permeability over 2.10×10^4 Barrer (91 % higher than that of pure PDMS membrane) and C_3H_8/N_2 selectivity of 99.5 (116 % higher than that of pure PDMS membrane) were achieved. Additionally, the as-prepared membrane also exhibited excellent stability during long term operation. © 2016 Curtin University of Technology and John Wiley & Sons, Ltd.

KEYWORDS: mixed matrix membranes; ZIF-8; hydrophobic functionalization; shell ligand exchange (SLE) reaction; hydrocarbon recovery

INTRODUCTION

Hydrocarbon is one of the most serious pollutants in urban life, which mainly remains in off-gas streams in gasoline station. It is necessary to recover hydrocarbons for protecting environment and human health.[1] Among different recovery technologies, membrane gas separation shows apparent advantages such as easy fabrication, low cost, and energy effectiveness.[2] The gas separation performance of membranes mainly depends on the membrane materials.[3,4] To date, glassy polymers (e.g. polyacetylenes [5] and polynorbornenes [6]) and rubbery polymers such as polydimethylsiloxane (PDMS) [7] are the major membrane materials applied in hydrocarbon recovery. Compared with other membrane materials, PDMS is a promising material to be used for separating hydrocarbons because of the high permeability, good chemical stability, and low cost. However, membranes of traditional polymeric materials including PDMS are often restricted by the swelling of chains, which results in the significant decrease of separation performance.[8–10]

Traditionally, polymeric membranes are restricted by trade-off effect, namely high selectivity and permeability are hard to be obtained simultaneously. In order to improve the membrane separation performance, mixed matrix membranes (MMMs) [4–11] were proposed and have attracted much attention. They combine the advantages of both the high performance of fillers and easy fabrication of polymeric membranes. Different organic or inorganic materials were investigated as dispersion phase to improve the performance of membranes, such as zeolite,[12–14] silica,[15] carbon nanotube,[16] graphene oxide, [17] and metal organic frameworks (MOFs).[18–20] Nowadays, MOFs have become one of the most popular materials for developing in MMMs,[21–26] owing to its high flexibility and tunable physicochemical properties. Zeolitic imidazolate framework (ZIF)-8, a typical member of ZIFs family, is formed by coordination of metal ions Zn^{2+} and 2-dimethyimidazole with a sodalite topological structure. It has been widely studied because of its

**Correspondence to*: Gongping Liu and Wanqin Jin, State Key Laboratory of Materials-Oriented Chemical Engineering, College of Chemistry and Chemical Engineering, Nanjing Tech University, 5 Xinmofan Road, Nanjing 210009, China. E-mail: gpliu@njtech.edu.cn; wqjin@njtech.edu.cn

unique molecular sieving structural pores, excellent thermal and chemical stability,[27] large surface area, and specific adsorption properties.[28] Additionally, it has been proved that ZIF-8 can exhibit much higher adsorption ability of hydrocarbons than that of nitrogen or other light gases.[29,30] As a result, ZIF-8 and its MMMs have shown great potential in gas separation especially the recovery of hydrocarbons.

Generally, the key factor for fully utilizing the functionality of fillers (e.g. ZIF-8) is to obtain desirable dispersibility in polymeric matrix. Li *et al*.[30] prepared ZIF-8 MMMs, but a limited selectivity was obtained. Physical methods like powerful sonication is usually applied; fillers aggregation cannot be completely avoided. Alternatively, chemical modification approaches are needed for further improving the interface compatibility between dispersion phase and polymeric matrix.[4] Our group developed surface grafting method to realize the homogenous dispersion of ZSM-5 zeolite in PDMS matrix,[31] which exhibited a good ethanol/water separation factor. Vankelecom *et al*.[32] used silylation treatment to modify zeolite to improve the fillers dispersion in the polymer. Also, Yi *et al*.[33] incorporated silicalite-1 modified by vinyltriethoxysilane (VTES) to prepare the silicalite-1/PDMS hybrid membrane. Chung *et al*.[34] incorporated ZIF-71 nanoparticles (<100 nm) boosted the molecular-sieving properties of tris (2-aminoethyl) amine-treated MMMs by constructing surface nanometric layer via vapor cross-linking.

In this work, ZIF-8 nanoparticles were effectively functionalized by 5,6-dimethylbenzimidazole (DMBIM) through shell ligand exchange (SLE) reaction. After functionalization, the ZIF-8-DMBIM nanoparticles became much more hydrophobic than pristine ZIF-8. For the first time, ZIF-8-DMBIM nanoparticles are introduced into PDMS matrix to prepare MMMs for propane/nitrogen separation. The schematic diagram describing the preparation of the SLE reaction was shown in Fig. S1 (ESI†). Additionally, the dispersibility of ZIF-8 nanoparticles in MMMs was effectively enhanced after surface functionalization by DMBIM. The as-prepared membranes with homogenously dispersed ZIF-8-DMBIIM nanoparticles are expected to effectively improve the separation performance of hydrocarbon. The effect of MOF nanoparticles loading on the gas separation performance as well as long-term operation test were also carried out and investigated.

EXPERIMENTAL SECTION

Materials

Polydimethylsiloxane (α, ω-dihydroxypolydimethylsiloxane, Mw = 60 000) was obtained from Shanghai Resin Factory Co., Ltd., China. Tetraethylorthosilicate, n-heptane, and dibutyltin dilaurate were supplied by Sinopharm Chemical Reagent Co., Ltd, China. Zinc nitrate hexahydrate (Zn, $Zn(NO_3)_2{\cdot}6H_2O$, 99%) was supplied by Aladdin and 2-methylimidazole (Hmin, $C_4H_6N_2$, 98%) was supplied by Sigma-Aldrich (USA). Methanol were purchased from Wuxi City Yasheng Chemical Co., Ltd (Wuxi, China). Poly(vinylidene fluoride) (PVDF) supports were purchased from Solvay (Cranbury, New Jersey, USA). All of the materials were used without further purification.

Synthesis of zeolitic imidazolate framework-8 and zeolitic imidazolate framework-8-5,6-dimethylbenzimidazole nanocrystals

Zeolitic imidazolate framework-8 nanocrystals were prepared according to the reported literature.[35] Typically, a solution of $Zn(NO_3)_2{\cdot}6H_2O$(2.933 g, 9.87 mmol) in 200 mL of methanol mixed with a solution of Hmim (6.489 g, 79.04 mmol) in 200 mL of methanol. Then, the mixed solution was stirring with a magnetic bar. After 1 h, the bulky solution are separated by centrifugation and washed with fresh methanol three times. Finally, crystals are dried at 40 °C in air.

Zeolitic imidazolate framework-8-DMBIM nanocrystals were prepared through SLE reaction.[36] DMBIM (5,6-dimethylbenzimidazole), methanol, trimethylamine, and treated ZIF-8 nanocrystals were dispersed in methanol in a Teflon container (mass ratio: ZIF-8-DMBIM-trimethylamine-MeOH = 1 : 1 : 0.7 : 160) and were stirred for 1 h. After that, it was taken into an oven at 60 °C for 15 h. The product was separated by centrifugation and washed with fresh methanol for later use. Finally, crystals are dried at 40 °C in air.

Fabrication of membrane

A certain amount of ZIF-8-DMBIM nanoparticles were dispersed in n-heptane and stirred for 30 min. Then, they were sonicated by probe-type sonicator (SCIENTZ, Ningbo, Zhejiang, China) at a power of 300 W for 30 min in an ice bath. PDMS polymer was uniformly dissolved in n-heptane, and then a certain amount of tetraethylorthosilicate and dibutyltin dilaurate were added into the mixed solution, respectively.[37] Then, ZIF-8-DMBIM nanoparticle suspensions were added into the beaker, and the resulting solution were stirred and cross-linked for another 5 h. Finally, the solution was casted on a PVDF substrate with a doctor blading. The resulted membrane was under the room temperature for 24 h to evaporate the guest molecule, and then dried in oven at 120 °C for 24 h. The thickness of the ZIF-8-DMBIM-PDMS MMMs ranged from 8 to 15 μm. ZIF-8-DMBIM loading of these MMMs was varied as 0, 5, 10, 20, and 30 wt%, respectively.

DOI: 10.1002/apj

Similarly, the unmodified ZIF-8 was incorporated into PDMS polymer to fabricate ZIF-8-PDMS MMMs as the control samples.

Characterization

The morphology of ZIF-8, ZIF-8-DMBIM nanoparticles and composite membranes were examined by field emission scanning electron microscope (FESEM, S4800, Hitachi, Japan). Nitrogen, propane adsorption and desorption isotherms (77 K) of ZIF-8 and ZIF-8DMBIM nanoparticles were carried out by thermogravimetric analysis (TGA, NETZSCH STA 449F3). Fourier transform infrared (FT-IR, Nicolet8700, Nicolet, USA) spectra were recorded in spectrophotometer with the range of 400–4000 cm^{-1}, using the KBr disk technique. ZIF-8 and ZIF-8-DMBIM nanocrystals were examined by X-ray diffractometer (XRD, Bruker, D8 Advance, Germany) using Cu Kα radiation, in the range of 5–50° with an increment of 0.5° at room temperature. The static contact angles of ZIF-8 and ZIF-8-DMBIM nanoparticles were characterized by contact angle measurement system (DSA100, Kruss, Germany) at room temperature. ZIF-8 and ZIF-8-DMBIM nanoparticle samples were processed into thin films, respectively. The results of contact angles were read within 30 s after depositing 8 μL of the probe liquid on the substrate. Each data point reported in this paper represents an average of five measurements on different areas of the same sample and has an error less than ±1.5°. Differential scanning calorimetry (DSC, Q2000, TA Instruments, USA) measurements were conducted from −130 to 20 °C in N_2 atmosphere.

Gas permeation test

Single gas permeation test was conducted to investigate the performance of the membrane by the method reported in our previous work.[38] The test was conducted via constant-pressure, variable-volume method with a transmembrane pressure of 0.3 MPa at the temperature of 25 °C. Gas flow rates were detected with a bubble flow meter. The specimen was cut into circular disks and mounted onto the home-made permeation cell. The effective permeation area of flat composite membrane was 4.91 cm^2.

It is well known that the mass transport in dense polymeric membranes follows the solution-diffusion mechanism. Each measurement was calculated at least five times. After the system reached steady state, we can use the following equation:

$$P = \frac{1}{\Delta p} \cdot \frac{273.15}{273.15 + T} \cdot \frac{1}{A} \cdot \frac{P_{atm}}{76} \cdot \left(\frac{dV}{dt}\right) \quad (1)$$

where P is the gas permeability [1 barrer = 10^{-10} cm^3 (STP) $cm/(cm^2 \cdot s \cdot cmHg)$], Δp is the transmembrane pressure (atm), p_{atm} is the atomospheric pressure (atm), and T is the room temperature (°C). A is the effective permeation area (cm^2), and dV/dt is the volumetric displacement rate in the bubble flow meter. The ideal separation factor which is the ratio of permeability of the individual gas can be expressed as follows:

$$\alpha = \frac{P_A}{P_B} \quad (2)$$

where P_A and P_B are the permeability of pure gas A and B, respectively.

RESULTS AND DISCUSSION

Morphologies of zeolitic imidazolate framework-8 and zeolitic imidazolate framework-8-5,6-dimethylbenzimidazole nanoparticles

As shown in Fig. 1, both of ZIF-8 and ZIF-8-DMBIM exhibited isometrical nanoparticles with narrow size distribution. All these nanoparticles are with the morphology of hexagonal envelope and sharp edges.[27] The average size of ZIF-8 nanoparticles is about 100 nm, while ZIF-8-DMBIM nanoparticles are with slightly larger particle size which can be due to the outside grafting of the shell made of DMBIM. Additionally, the size distribution of ZIF-8-DMBIM nanoparticles was shown in Fig. S2 (ESI†). The static contact angle images of water droplets for ZIF-8 and ZIF-8-DMBIM nanoparticles were shown in the inserted in Fig. 1a and b. Compared with ZIF-8 nanoparticles, ZIF-8-DMBIM nanoparticles showed a significant increase of the contact angle from 67° to 123°, suggesting the hydrophobicity of the DMBIM shell outside the ZIF-8 nanoparticles. XRD patterns of ZIF-8 and ZIF-8-DMBIM nanocrystals are shown in Fig. 2, which indicate typical crystalline ZIF-8 structure (sodalite topology).[39] It confirms that after surface functionalization, the ZIF-8-DMBIM nanoparticles can still retain the original crystal structure.

Physicochemical properties of zeolitic imidazolate framework-8 and zeolitic imidazolate framework-8-5,6-dimethylbenzimidazole nanoparticles

The DMBIM grafting of ZIF-8 nanoparticles was further verified by FT-IR spectra. The range of wavenumber is from 700–800 and 3055–3300 cm^{-1}.

DOI: 10.1002/apj

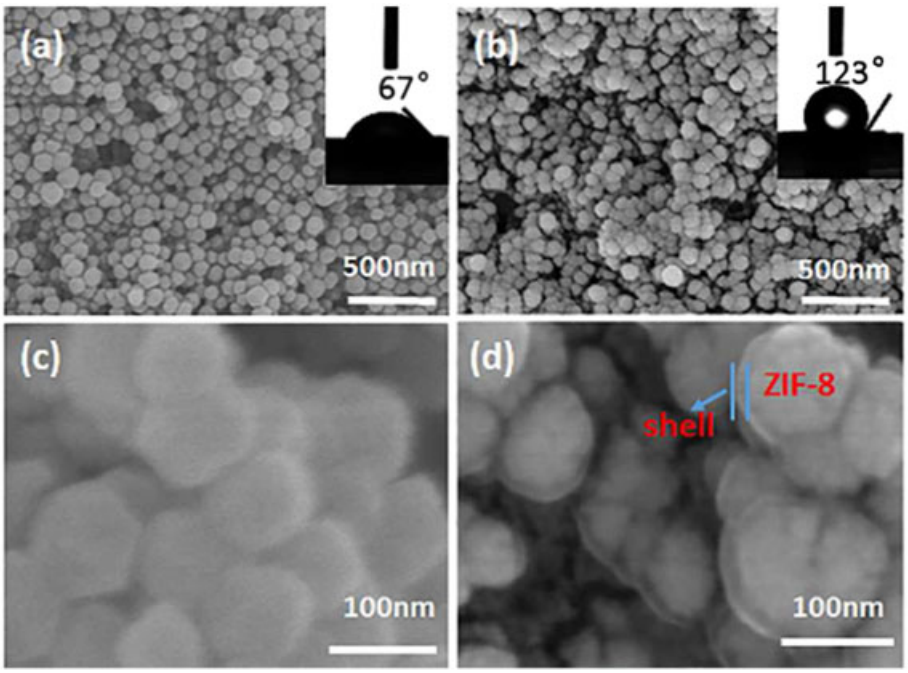

Figure 1. Field emission scanning electron microscope (FESEM) images of (a) zeolitic imidazolate framework (ZIF)-8 and (b) ZIF-8-DMBIM nanocrystals. The insets are the static contact angle images of water droplets corresponding to the FESEM images. (c) and (d) are the FESEM images at higher magnification of ZIF-8 and ZIF-8-5,6-dimethylbenzimidazole nanocrystals, respectively.

Compared with ZIF-8 nanoparticles, the spectrum of ZIF-8-DMBIM nanoparticle appears two new peaks at about 815 and 850 cm^{-1}, which are corresponding to the C-H out-of-plane deformation vibrations of the phenyl rings in DMBIM (Fig. 3a). It suggests that DMBIM has been grafted onto the ZIF-8. Furthermore, the broad band N-H stretching vibrations disappeared at 3100 cm^{-1} and a red shift at around 840 cm^{-1}, which can be explained by the process of deprotonation-coordination. [36] Thermogravimetric analysis (TG) curves of ZIF-8 and ZIF-8-DMBIM nanoparticles are shown in Fig. 3b to analyze the thermal properties. Both of ZIF-8 and ZIF-8-DMBIM nanoparticles showed the mass fraction decreased at about 600 °C. ZIF-8-DMBIM nanoparticles remain good thermal stability, because they show similar TG curves with that of ZIF-8 nanoparticles. N_2 sorption isotherm (77 K) and pore size analysis of ZIF-8 and ZIF-8-DMBIM nanoparticles are shown in Fig. 4a. Because of existence of micropores, a rapid volume increase of adsorption at low relative pressure can be observed. The following uptake at high relative pressure is due to the existence of structured macropores formed by incomplete packing of nanoparticles. The isotherm curves (both adsorption and desorption branches) of ZIF-8-DMBIM are consistent with that of ZIF-8 nanoparticles. ZIF-8 is a highly porous material, which enables it a high Brunner–Emmet–Teller (BET) surface areas. After SLE reaction, there appeared a slight decrease in BET surface area (from 1527.9 to 1224.5 m^2/g) because of the DMBIM shell outside the ZIF-8 nanoparticles. The inset of Fig. 4a shows pore size distribution between ZIF-8 and ZIF-8-DMBIM nanoparticles.

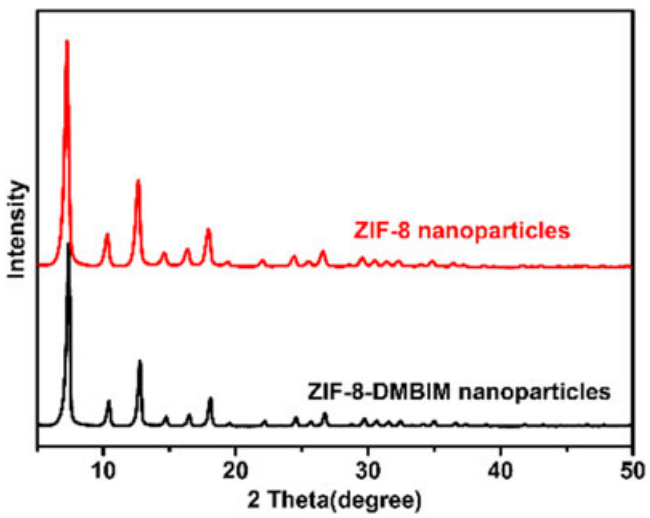

Figure 2. XRD patterns of zeolitic imidazolate framework-8 (ZIF-8) and zeolitic imidazolate framework-5,6-dimethylbenzimidazole (ZIF-DMBIM) nanoparticles, respectively.

We also measured gas adsorption properties (C_3H_8 and N_2) of ZIF-8 and ZIF-8-DMBIM at room temperature. As is shown in Fig. 4b, the maximum uptake amount for C_3H_8 of ZIF-8 nanoparticle is 7

DOI: 10.1002/apj

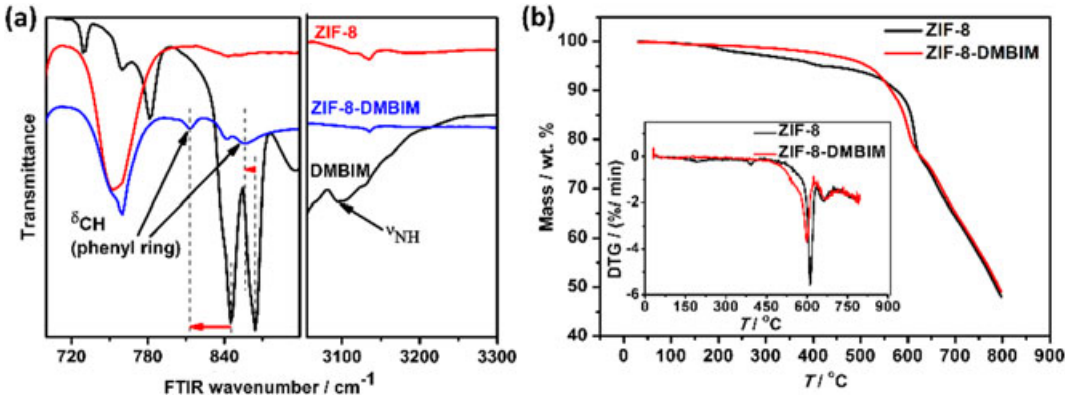

Figure 3. (a) Fourier transform infrared (FTIR) spectra of zeolitic imidazolate framework (ZIF)-8(red), 5,6-dimethylbenzimidazole (DMBIM) (black), and ZIF-8-DMBIM (blue). (b) TG curves of ZIF-8 (black) and ZIF-8-DMBIM (red) nanoparticles. The insets are the Derivative thermogravimetric analysis (DTG) images of ZIF-8 (black) and ZIF-8-DMBIM nanoparticles (red), respectively.

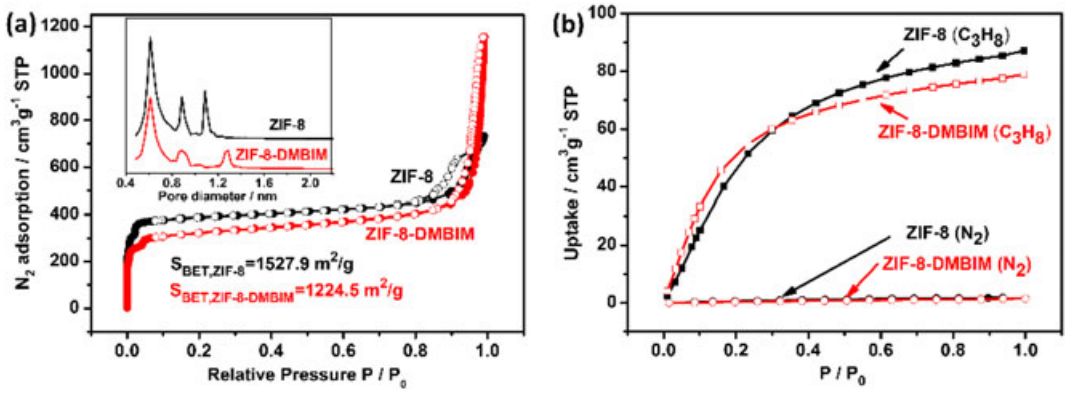

Figure 4. The N2 adsorption and isotherm (77 K) and (inset) pore size analysis of zeolitic imidazolate framework (ZIF)-8(black) and ZIF-8-5,6-dimethylbenzimidazole (DMBIM) (red). (b) N2 and C3H8 adsorption and desorption isotherms of ZIF-8 and ZIF-8-DMBIM nanoparticles at room temperature (25 °C).

times higher than that of N_2. The same characteristic is observed in ZIF-8-DMBIM nanoparticles. This is owing to the high adsorption selectivity of C_3H_8/N_2 of the ZIF-8 nanoparticles. The gas adsorption of ZIF-8-DMBIM nanoparticles decreased a little because of the minor decrease in BET surface area. At the pressure of 0.1 MPa, C_3H_8/N_2 adsorption selectivity of ZIF-8-DMBIM (55.2) is slightly higher than that of ZIF-8 nanoparticles (47.8). The result indicates that SLE reaction modification of DMBIM did not damage the 3D framework of ZIF-8 and maintain good adsorption ability for propane. Additionally, the SLE reaction increases the amount of organic ligands of ZIF-8 nanoparticles, which can enhance the compatibility between ZIF-8 filler and polymer matrix. Therefore, we expected that the incorporation of ZIF-8-DMBIM nanoparticles with preferential C_3H_8 adsorption property into PDMS matrix can realize fast and selective transport for C_3H_8 molecules.

Membrane characterization

Morphologies

Figures 5a–b show the FESEM images of PVDF supported pure PDMS membranes. The surface of pure PDMS membrane is very smooth without defects. The PDMS layer adheres well to the support layer. SEM images of membrane with 10 wt% ZIF-8 loading (Fig. 5c–d) show that the surface of the membrane appeared many bulges, whose sizes are larger than the particle size of ZIF-8, indicating that ZIF-8 nanoparticles were severely agglomerated in the PDMS matrix. Surface and cross-sectional morphology of ZIF-8-PDMS membranes with different ZIF-8 loading were shown in Fig. S3 (ESI†). With the increase of ZIF-8 nanoparticles loading, the aggregation becomes more significant. Meanwhile, FESEM images of membranes at 10 wt% ZIF-8-DMBIM loading (Fig. 5e–f) show that the ZIF-8-DMBIM nanoparticles were closely embedded in the PDMS matrix with no

DOI: 10.1002/apj

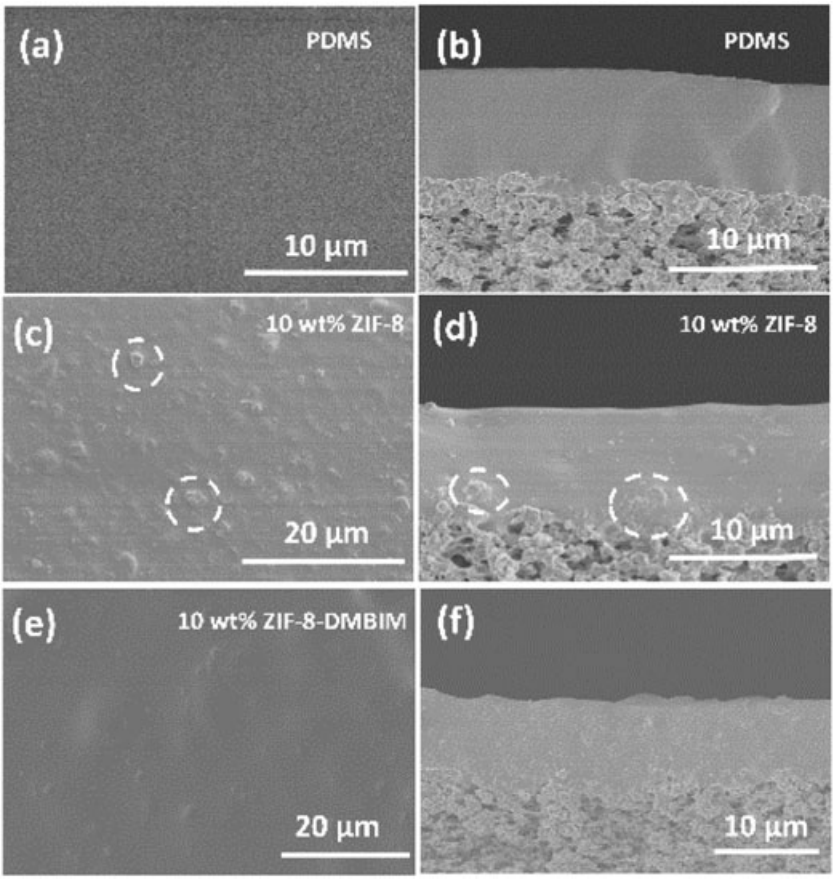

Figure 5. Field emission scanning electron microscope images of the (a) surface and (b) cross-section of polydimethylsiloxane (PDMS) membrane. (c) Surface and (d) cross-section of zeolitic imidazolate framework (ZIF)-8/PDMS membrane with ZIF-8 loading of 10 wt%; (e) Surface and (f) cross-section of ZIF-8-5,6-dimethylbenzimidazole (DMBIM)/PDMS membrane with ZIF-8-DMBIM loading of 10 wt%. White dashed cycles indicate the aggregation of metal organic framework particles.

voids. In contrast to the ZIF-8 particles in Fig. 5c–d, the ZIF-8-DMBIM nanoparticles were dispersed homogeneously in the PDMS matrix. This is because that the DMBIM shell endows ZIF-8-DMBIM additional organic ligands that improves the interfacial compatibility between MOFs nanoparticles and

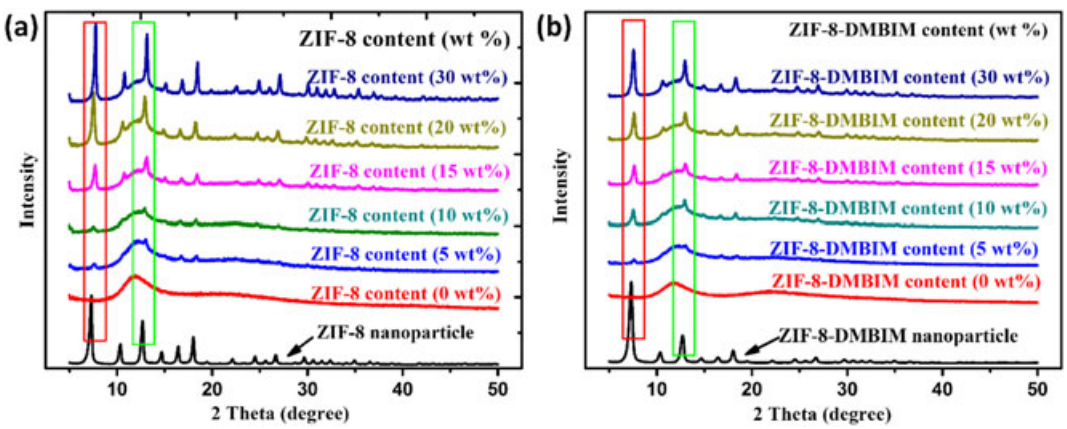

Figure 6. X-ray diffractometer patterns of (a) zeolitic imidazolate framework (ZIF)-8-polydimethylsiloxane and (b) ZIF-8-5,6-dimethylbenzimidazole (DMBIM)-polydimethylsiloxane mixed matrix membranes with different loadings.

DOI: 10.1002/apj

polymer chains. The morphology of ZIF-8-DMBIM-PDMS membranes with different ZIF-8-DMBIM loadings are shown in Fig. S4 (ESI†).

Microstructure

X-ray diffractometer patterns of ZIF-8-PDMS and ZIF-8-DMBIM-PDMS MMMs with different loadings are shown in Fig. 6. A broad diffraction was found at around 13°, corresponding to the cross-linked PDMS. The intensity of the PDMS peak increased with the ZIF-8-DMBIM loading, which may due to the increased thickness of membranes. Therefore, the peak intensity ratio of ZIF-8 (at 7°) to PDMS (at about 13°) and ZIF-8-DMBIM (at 7°) to PDMS (at about 13°) were calculated to eliminate the influence of membrane thickness, respectively. Figure 6 shows that the peak intensity ratios of both ZIF-8 and ZIF-8-DMBIM to PDMS increased proportionally with MOFs content. This result demonstrates that the physical incorporation of ZIF-8 and ZIF-8-DMBIM in PDMS matrix, which would not destroy the network of cross-linked PDMS network.

Fourier transform infrared spectra of ZIF-8, ZIF-8-DMBIM nanoparticles, ZIF-8-PDMS, and ZIF-8-DMBIM-PDMS MMMs are presented in Fig. 7. Typically, Si-O-Si asymmetric stretching vibration (1080 and 1010 cm^{-1}) and Si-O-Si symmetric stretching vibration (1080 and 1010 cm^{-1}) are consistent with chemical structure of the PDMS. It seems that the characteristic peak of ZIF-8-DMBIM nanoparticles did not appear in the spectra of ZIF-8-DMBIM-PDMS MMMs, because it was overlapped with the characteristic peaks of PDMS matrix. The spectra of ZIF-8-DMBIM-PDMS MMMs with different loadings did not appear with new characteristic peaks, indicating that there is no chemical reaction during the incorporation process. This is also in agreement with the analysis of XRD patterns. Similar features are also observed in the spectra of ZIF-8 MMMs.

Thermal properties of mixed matrix membranes

Thermogravimetric analysis was carried out to further investigate the thermal properties of MMMs. As shown in Fig. 8a, the degradation point of pure PDMS membrane is about 398 °C. Meanwhile, ZIF-8-PDMS (10 wt%) and ZIF-8-DMBIM-PDMS (10 wt%) MMMs both showed an excellent stability with a higher degradation temperature (>440 °C), which indicates that the thermal stability were enhanced by incorporating ZIF-8 nanoparticles. Moreover, the glass transition temperature (T_g) is an important parameter to estimate the chain rigidity of polymer materials. Table 1 lists the T_g of pure PDMS membrane and ZIF-8-DMBIM-PDMS membranes with different loadings. With increasing ZIF-8-DMBIM nanoparticles loading from 0 to 5 wt%, T_g increased sharply from −133.4 to −121.8 °C. This can be owing to the strong MOF-polymer interaction by interfacial functionalized by DMBIM. Further increasing the loading of ZIF-8-DMBIM nanoparticles from 5 to 20 wt%, T_g remains almost unchanged because of gradual aggregation of MOFs particles at high nanoparticle loadings. The polymer chain rigidification near the MOFs surface probably resulted from the inhibited isotropic contraction of the polymer. When the loading of ZIF-8-DMBIM nanoparticles is increased to 30 wt%, *Tg* increased again to −118.7 °C. The aggregation of MOFs particles increased the contact area between the particle and polymer chain, which have a more effect on the inhibition of the polymer contraction, thus leading to a larger thickness of rigidified polymer region.[40]

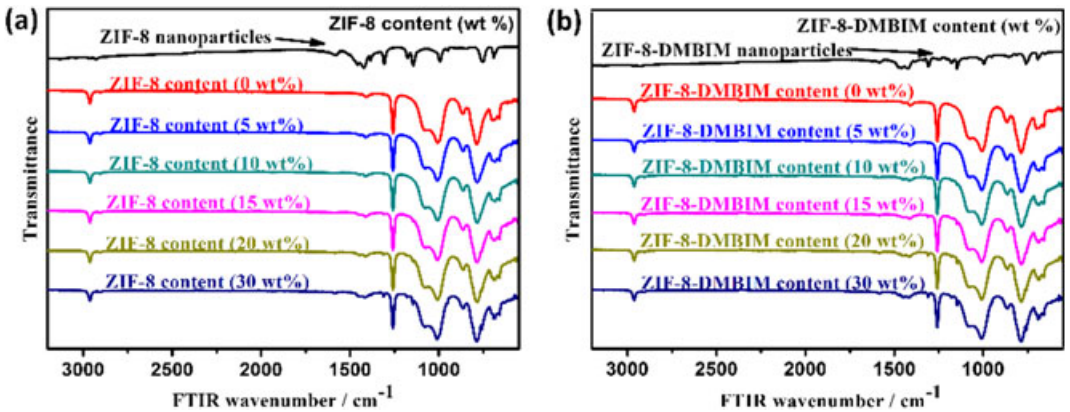

Figure 7. Fourier transform infrared (FTIR) spectra of (a) ZIF-8 nanoparticle zeolitic imidazolate framework-8-polydimethylsiloxane (ZIF-8-PDMS) mixed matrix membranes with different loading and (b) ZIF-8-5,6-dimethylbenzimidazole (DMBIM) nanoparticle, ZIF-8-DMBIM-PDMS mixed matrix membranes with different loadings.

DOI: 10.1002/apj

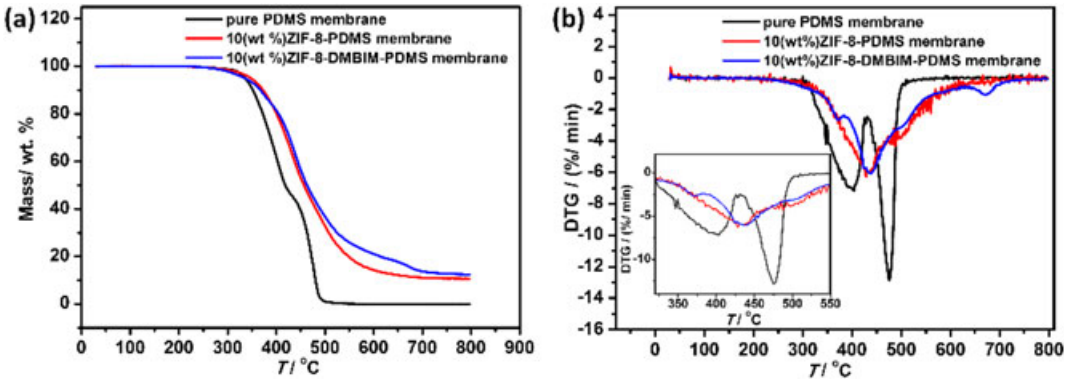

Figure 8. (a) TG and (b) DTG curves of pure polydimethylsiloxane (PDMS) membrane, 10 (wt %) zeolitic imidazolate framework (ZIF)-8-PDMS and 10 (wt %) ZIF-8-(5,6-dimethylbenzimidazole) DMBIM-PDMS MMMs. The inset of (b) is the magnification of the degradation of point.

Table 1. *Tg* of pure PDMS membrane and ZIF-8-DMBIM-PDMS membranes with different loadings.

ZIF-8-DMBIM content (wt%)	*Tg* (°C)
0	−133.1
5	−123.8
10	−122.6
20	−122.1
30	−118.6

PDMS, polydimethylsiloxane;ZIF-8, zeolitic imidazolate framework-8; DMBIM, 5,6-dimethylbenzimidazole.

Mechanical property

Theoretically, the hardness belongs to an intrinsic property of materials. It is useful to map the distribution of hardness across a large membrane area so as to check the uniformity of MMMs. If there are fillers in the matrix, it will make the chain of matrix rigidified, thus to restrict the chain mobility. As is shown from Fig. 9, the harness distribution of 10 wt% ZIF-8-DMBIM-PDMS MMMs is relatively smoother than 10 wt% ZIF-8-PDMS MMMs. The hardness distributions of ZIF-8-PDMS and ZIF-8-DMBIM-PDMS MMMs with different loadings are shown in Fig. S4 and S5 (ESI†), all indicating that ZIF-8-DMBIM-PDMS MMMs can show better hardness distribution. As shown in Fig. S6 (ESI†), by increasing the loading of ZIF-8 and ZIF-8-DMBIM nanoparticles, the hardness of the MMM increased gradually. It is due to the molecular interactions between nanoparticles and PDMS matrix. Compared with ZIF-8-PDMS MMMs, the hardness of ZIF-8-PDMS-DMBIM MMMs were larger than those of the former one. It is due to the rigidity and abundant ligand of ZIF-8-DMBIM, which makes the better dispersion in the PDMS matrix. The result of nano-scratch test also agrees well with the variation of T_g.

Gas permeation

Solution-diffusion mechanism is applied in dense polymeric membranes.[41] In glassy, rigid polymers, such as polysulphone, permeant diffusion coefficient is more important than its solubility coefficient. Therefore, these polymers preferentially permeate the smaller, less condensable gases, H_2 and CH_4 over the larger, more condensable gases, C_3H_8 and CO_2. While in rubbery polymers such as PDMS, permeant solubility coefficients are the dominant factor. Thus, these polymers preferentially permeate the larger, more

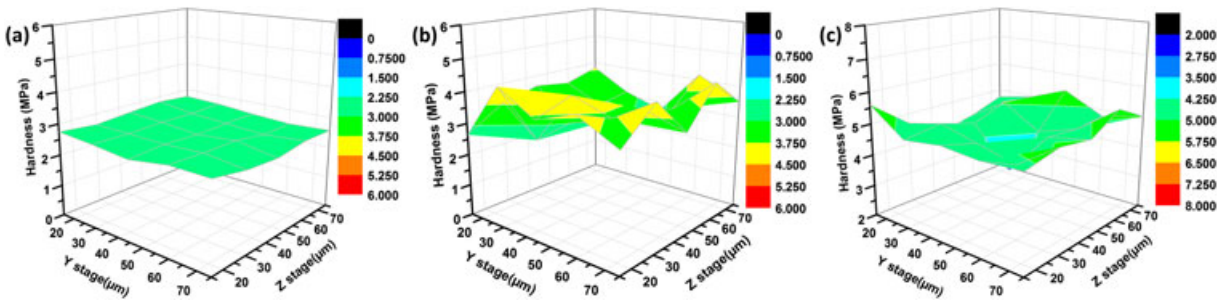

Figure 9. Distribution of hardness of (a) pure polydimethylsiloxane (PDMS) membrane; (b) 10 wt% zeolitic imidazolate framework-8-PDMS mixed matrix membranes; (c) 10 wt% zeolitic imidazolate framework-8-5,6-dimethylbenzimidazole-PDMS mixed matrix membranes.

DOI: 10.1002/apj

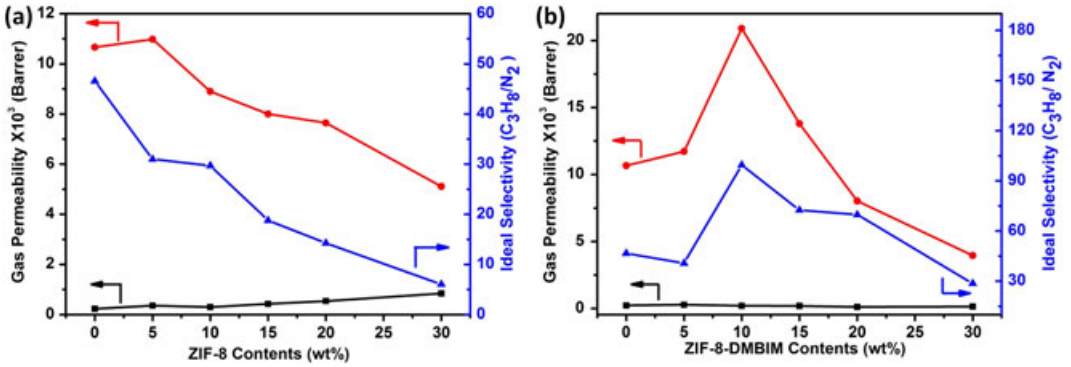

Figure 10. Effect of (a) zeolitic imidazolate framework-8 (ZIF-8) loading and (b) zeolitic imidazolate framework-8-5,6-dimethylbenzimidazole (ZIF-8-PDMS) on separation factor and selectivity. The gas permeation tests were measured at 0.3 MPa and 25 C, 1 Barrer =10^{-10} cm^3(STP) cm/(cm^2 s cmHg).

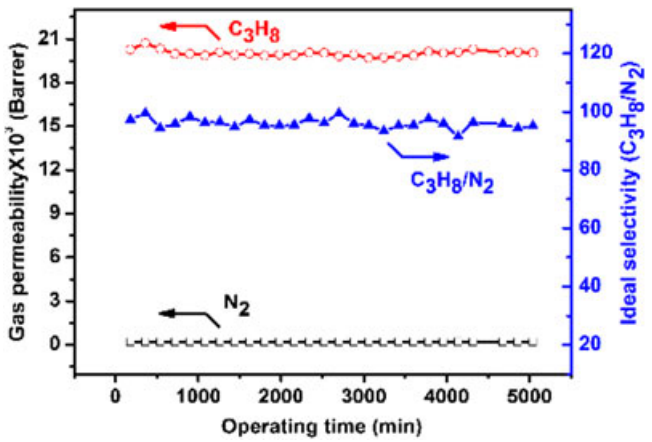

Figure 11. Long-term operation test of C3H8/N2 for zeolitic imidazolate framework-8-5,6-dimethylbenzimidazole-polydimethylsiloxane membrane with 10 wt% loading.

condensable gases over the smaller, less condensable gases.[42] For ZIF-8-PDMS MMMs (Fig. 10a), when the loading rises to 5 wt%, a maximum C_3H_8 permeability reaches to 10 985 Barrer. With the increase of ZIF-8 nanoparticles, C_3H_8/N_2 selectivity decreased gradually, which is due to of the microdefects caused by the aggregation of ZIF-8 nanoparticles. The C_3H_8 permeability is also decreased with the ZIF-8 loading. It might be due to the aggregation of ZIF-8 nanoparticles in polymeric matrix, resulting in highly strong adsorption of C_3H_8 molecules, which cannot be easily desorbed according to the Maxwell model.[31] Obviously, this fillers aggregation in polymeric matrix is not beneficial for enhancing the membrane separation performance. Hence, interfacial functionalization of ZIF-8 nanoparticles was applied to improve the dispersion of ZIF-8 nanoparticles in PDMS membrane. As shown in Fig. 10b, with the increasing of the ZIF-8-DMBIM loading, both the C_3H_8 permeability and selectivity are significantly increased. When the loading increases to 10 wt%, a maximum C_3H_8 permeability (2.10×10^4 Barrer) appears coupled with a maximum ideal selectivity (99.5). As proved above, ZIF-8-DMBIM possesses more organic ligands and higher hydrophobicity than ZIF-8, which favors the interfacial compatibility with PDMS chains. It improved the dispersion of ZIF-8-DMBIM nanoparticles in the polymer matrix, inhibiting the generation of microdefects. With further increasing the ZIF-8-DMBIM nanoparticles to more than 10 wt%, the C_3H_8 permeability and selectivity were decreased, which is due to the gradually aggregation of ZIF-8-DMBIM nanoparticles.

Long-term operation test

The pure PDMS membrane was reported to show a relatively low separation factor after a long operation test.[7,8] It is generally due to the excessive membrane swelling caused by the continuous uptake of gas. We conducted a continuous gas permeation for more than 5000 min for ZIF-8-DMBIM membrane with loading of 10 wt% to investigate the long-term operation stability (Fig. 11). It turns out that no defects were found in ZIF-8-DMBIM-PDMS membrane after the long-term operation, suggesting a good membrane structural stability. It can be expected that the prepared membrane is feasible and promising for practical application in future.

CONCLUSIONS

In this work, ZIF-8-DMBIM-PDMS MMMs have been firstly developed for hydrocarbon separation. ZIF-8-DMBIM nanoparticles were synthesized with more organic ligands by hydrophobically functionalization (SLE reaction), meanwhile maintaining the original crystal structure and physicochemical properties of ZIF-8. The as-prepared ZIF-8-DMBIM-PDMS MMMs showed better dispersion of MOFs particles than that of ZIF-8-PDMS membranes. By incorporating 10 wt%

DOI: 10.1002/apj

ZIF-8-DMBIM, the PDMS MMMs exhibited high C_3H_8 permeability of 2.10×10^4 Barrer (91% higher than that of pure PDMS membrane) and the C_3H_8/N_2 selectivity of 99.5 (116% higher than that of pure PDMS membrane). Our work demonstrated that the ZIF-8-DMBIM-PDMS MMMs is a promising candidate for the application of hydrocarbons recovery. Moreover, this new strategy of interfacial functionalization of MOFs nanoparticles is believed to be useful for developing high performance MMMs with broad applications such as gas separation and water purification.

Author Contributions

Wanqin Jin, Gongping Liu and Jianwei Yuan conceived the experiments. Jianwei Yuan prepared the membrane and carried out most of the characterization. The manuscript was discussed and written through contributions of all authors. All authors have given approval to the final version of the manuscript.

CONFLICT OF INTEREST

The authors declare no competing financial interest.

Acknowledgements

This work was financially supported by the National Natural Science Foundation of China (grant nos. 21406107, 21490585, 21301148), the Innovative Research Team Program by the Ministry of Education of China (grant no. IRT13070), the Natural Science Foundation of Jiangsu Province (no. BK20140930), Topnotch Academic Programs Project of Jiangsu Higher Education Institutions (TAPP), and the Innovation Project of Graduate Research by Jiangsu Province (grant no. KYLX_0764).

REFERENCES

[1] Baker RW, Wijmans JG, Kaschemekat JH. The design of membrane vapor–gas separation systems. *J. Membrane. Sci.* 1998; **151**: 55–62.
[2] Bernardo P, Drioli E, Golemme G. Membrane gas separation: a review/state of the art. *Industrial and Engineering Chemistry Research* 2009; **48**: 4638–4663.
[3] Merkel TC, Freeman BD, Spontak RJ, He Z, Pinnau I, Meakin P, Hill AJ. Ultrapermeable, reverse-selective nanocomposite membranes. *Science* 2002; **296**: 519–522.
[4] Chung TS, Jiang LY, Li Y, Kulprathipanja S. Mixed matrix membranes (MMMs) comprising organic polymers with dispersed inorganic fillers for gas separation. *Progress in Polymer Science* 2007; **32**: 483–507.
[5] Merkel TC, Bondar VI, Nagai K, Freeman BD. Sorption and transport of hydrocarbon and perfluorocarbon gases in poly(1-trimethylsilyl-1-propyne). *J. Polym. Sci. Pol. Phys.* 2000; **38**: 273–296.
[6] Starannikova L, Pilipenko M, Belov N, Yampolskii Y, Gringolts M, Finkelshtein E. Addition-type polynorbornene with $Si(CH_3)_3$ side groups: detailed study of gas permeation and thermodynamic properties. *J. Membrane. Sci.* 2008; **323**: 134–143.
[7] Merkel TC, Bondar VI, Nagai K, Freeman BD, Pinnau I. Gas sorption, diffusion, and permeation in poly(dimethylsiloxane). *J. Polym. Sci. Pol. Phys.* 2000; **38**: 415–434.
[8] Jiang X, Kumar A. Performance of silicone-coated polymeric membrane in separation of hydrocarbons and nitrogen mixtures. *J. Membrane. Sci.* 2005; **254**: 179–188.
[9] Shi Y, Burns CM, Feng X. Poly(dimethyl siloxane) thin film composite membranes for propylene separation from nitrogen. *J. Membrane. Sci.* 2006; **282**: 115–123.
[10] Ghadimi A, Sadrzadeh M, Shahidi K, Mohammadi T. Ternary gas permeation through a synthesized PDMS membrane: Experimental and modeling. *J. Membrane. Sci.* 2009; **344**: 225–236.
[11] Zimmerman CM, Singh A, Koros WJ. Tailoring mixed matrix composite membranes for gas separations. *J. Membrane. Sci.* 1997; **137**: 145–154.
[12] Snyder MA, Tsapatsis M. Hierarchical nanomanufacturing: from shaped zeolite nanoparticles to high-performance separation membranes. *Angew. Chem. Int. Edit.* 2007; **46**: 7560–7573.
[13] Vane LM, Namboodiri VV, Bowen TC. Hydrophobic zeolite–silicone rubber mixed matrix membranes for ethanol–water separation: effect of zeolite and silicone component selection on pervaporation performance. *J. Membrane. Sci.* 2008; **308**: 230–241.
[14] Dobrak A, Figoli A, Chovau S, Galiano F, Simone S, Vankelecom IFJ, Drioli E, Van der Bruggen B. Performance of PDMS membranes in pervaporation: effect of silicalite fillers and comparison with SBS membranes. *J. Colloid. Interf. Sci.* 2010; **346**: 254–264.
[15] Ahn J, Chung W-J, Pinnau I, Guiver MD. Polysulfone/silica nanoparticle mixed-matrix membranes for gas separation. *J. Membrane. Sci.* 2008; **314**: 123–133.
[16] Bose S, Khare RA, Moldenaers P. Assessing the strengths and weaknesses of various types of pre-treatments of carbon nanotubes on the properties of polymer/carbon nanotubes composites: a critical review. *Polymer* 2010; **51**: 975–993.
[17] Shen J, Liu G, Huang K, Jin W, Lee KR, Xu N. Membranes with fast and selective gas-transport channels of laminar graphene oxide for efficient CO2 capture. *Angew. Chem. Int. Edit.* 2014; **54**: 578–582.
[18] Ordonez MJC, Balkus KJ, Ferraris JP, Musselman IH. Molecular sieving realized with ZIF-8/Matrimid (R) mixed-matrix membranes. *J. Membrane. Sci.* 2010; **361**: 28–37.
[19] Eddaoudi M, Li HL, Yaghi OM. Highly porous and stable metal–organic frameworks: Structure design and sorption properties. *Journal of the American Chemical Society* 2000; **122**: 1391–1397.
[20] Japip S, Xiao YC, Chung T-S. Particle size effects on gas transport properties of 6FDA-Durene/ZIF-71 mixed matrix membranes. *Industrial and Engineering Chemistry Research* 2016; **55**: 9507–9517.
[21] Perez EV, Balkus KJ, Ferraris JP, Musselman IH. Mixed-matrix membranes containing MOF-5 for gas separations. *J. Membrane. Sci.* 2009; **328**: 165–173.
[22] Adams R, Carson C, Ward J, Tannenbaum R, Koros W. Metal organic framework mixed matrix membranes for gas separations. *Micropor. Mesopor. Mat.* 2010; **131**: 13–20.
[23] Basu S, Cano-Odena A, Vankelecom IFJ. Asymmetric Matrimid (R)/$Cu_3(BTC)_2$ mixed-matrix membranes for gas separations. *J. Membrane. Sci.* 2010; **362**: 478–487.
[24] Dai Y, Johnson JR, Karvan O, Sholl DS, Koros WJ. Ultem(R)/ZIF-8 mixed matrix hollow fiber membranes for CO_2/N_2 separations. *J. Membrane. Sci.* 2012; **401**: 76–82.
[25] Jeazet HBT, Staudt C, Janiak C. Metal–organic frameworks in mixed-matrix membranes for gas separation. *Dalton. T.* 2012; **41**: 14003–14027.
[26] Yao J, Wang H. Zeolitic imidazolate framework composite membranes and thin films: synthesis and applications. *Chemical Society Reviews* 2014; **43**: 4470–4493.

[27] Park KS, Ni Z, Cote AP, Choi JY, Huang R, Uribe-Romo FJ, Chae HK, O'Keeffe M, Yaghi OM. Exceptional chemical and thermal stability of zeolitic imidazolate frameworks. *P. Natl. Acad. Sci. USA.* 2006; **103**: 10186–10191.
[28] Shi GM, Yang T, Chung TS. Polybenzimidazole (PBI)/ zeolitic imidazolate frameworks (ZIF-8) mixed matrix membranes for pervaporation dehydration of alcohols. *J. Membrane. Sci.* 2012; **415–416**: 577–586.
[29] Zhang K, Lively RP, Zhang C, Chance RR, Koros WJ, Sholl DS, Nair S. Exploring the framework hydrophobicity and flexibility of zif-8: from biofuel recovery to hydrocarbon separations. *Journal of Physical Chemistry Letters* 2013; **4**: 3618–3622.
[30] Fang M, Wu C, Yang Z, Wang T, Xia Y, Li J. ZIF-8/PDMS mixed matrix membranes for propane/nitrogen mixture separation: experimental result and permeation model validation. *J. Membrane. Sci.* 2015; **474**: 103–113.
[31] Liu G, Xiangli F, Wei W, Liu S, Jin W. Improved performance of PDMS/ceramic composite pervaporation membranes by ZSM-5 homogeneously dispersed in PDMS via a surface graft/coating approach. *Chemical Engineering Journal* 2011; **174**: 495–503.
[32] Vankelecom IFJ, VandenBroeck S, Merckx E, Geerts H, Grobet P, Uytterhoeven JB. Silylation to improve incorporation of zeolites in polyimide films. *The Journal of Physical Chemistry* 1996; **100**: 3753–3758.
[33] Yi S, Su Y, Wan Y. Preparation and characterization of vinyltriethoxysilane (VTES) modified silicalite-1/PDMS hybrid pervaporation membrane and its application in ethanol separation from dilute aqueous solution. *J. Membrane. Sci.* 2010; **360**: 341–351.
[34] Japip S, Liao K-S, Xiao YC, Chung T-S. Enhancement of molecular-sieving properties by constructing surface nano-metric layer via vapor cross-linking. *J. Membrane. Sci.* 2015; **497**: 248–258.
[35] Cravillon J, Münzer S, Lohmeier S-J, Feldhoff A, Huber K, Wiebcke M. Rapid room-temperature synthesis and characterization of nanocrystals of a prototypical zeolitic imidazolate framework. *Chemistry of Materials* 2009; **21**: 1410–1412.
[36] Liu X, Li Y, Ban Y, Peng Y, Jin H, Bux H, Xu L, Caro J, Yang W. Improvement of hydrothermal stability of zeolitic imidazolate frameworks. *Chemical Communications* 2013; **49**: 9140–9142.
[37] Xiangli F, Chen Y, Jin W, Xu N. Polydimethylsiloxane (PDMS)/ceramic composite membrane with high flux for pervaporation of ethanol-water mixtures. *Industrial and Engineering Chemistry Research* 2007; **46**: 2224–2230.
[38] Huang K, Dong X, Ren R, Jin W. Fabrication of homochiral metal–organic framework membrane for enantioseparation of racemic diols. *AICHE Journal* 2013; **59**: 4364–4372.
[39] Cravillon J, Nayuk R, Springer S, Feldhoff A, Huber K, Wiebcke M. Controlling zeolitic imidazolate framework nano- and microcrystal formation: insight into crystal growth by time-resolved in situ static light scattering. *Chemistry of Materials* 2011; **23**: 2130–2141.
[40] Li Y, Guan H-M, Chung T-S, Kulprathipanja S. Effects of novel silane modification of zeolite surface on polymer chain rigidification and partial pore blockage in polyethersulfone (PES)–zeolite. A mixed matrix membranes. *J. Membrane. Sci.* 2006; **275**: 17–28.
[41] Wijmans JG, Baker RW. The solution-diffusion model: a review. *J. Membrane. Sci.* 1995; **107**: 1–21.
[42] Sadrzadeh M, Shahidi K, Mohammadi T. Preparation and C_3H_8/gas separation properties of a synthesized single layer pdms membrane. *Separation Science and Technology* 2010; **45**: 592–603.

SUPPORTING INFORMATION

Additional supporting information may be found in the online version of this article at publisher's website.

DOI: 10.1002/apj